Research Article Vol. 56, No. 33 / November 20 2017 / Applied Optics 9233

applied optics

Analysis and reduction of the TDI CCD charge transfer image shift

YUN-HUI LI,[1,2,*] XIAO-DONG WANG,[1] WEN-GUANG LIU,[1] AND ZHI WANG[3]

[1]Changchun Institute of Optics, Fine Mechanics and Physics, Chinese Academy of Sciences, Changchun 130033, China
[2]University of Chinese Academy of Sciences, Beijing 100049, China
[3]Changchun UP Optotech (Holding) Co., Ltd., Changchun 130033, China
*Corresponding author: liyunhui_ciomp@126.com

Received 13 July 2017; revised 9 October 2017; accepted 18 October 2017; posted 19 October 2017 (Doc. ID 302312); published 14 November 2017

Based on the description of the charge transfer process of a time delay integration charge coupled device (TDI CCD), it is pointed out that the relative displacement of the target image and the transferred charge introduces the charge transfer image shift problem in a line transfer period, which leads to the decrease of the modulation transfer function (MTF) in the scanning direction. Based on the basic definition of MTF, the charge transfer image shift model of the TDI CCD is established. According to the quantitative calculation of this model, the MTF curves of the three-phase TDI CCD are obtained under the condition of different pulse widths of computer interface (CI) signals. The MTF changes with the pulse width of CI signals, and the maximum value at the spatial Nyquist frequency is obtained when the CI signals are equally spaced, which is difficult to achieve in the actual system because of the limitation of computed radiography readout signals. In this paper, we present the improved TDI CCD driving timing, which makes it possible to realize the equal interval distribution of CI signals by adjusting the technology compatibility kit signal. Finally, the experimental platform is built, and the MTF curves are calculated from the obtained target images. The result is consistent with the theoretical model.

OCIS codes: (040.0040) Detectors; (110.0110) Imaging systems; (280.0280) Remote sensing and sensors; (040.1520) CCD, charge-coupled device.

https://doi.org/10.1364/AO.56.009233

1. INTRODUCTION

The time delay integration (TDI) charge coupled device (CCD) has multiple exposures to the same target by means of TDI, boosting the exposure time and allowing more photons to be collected. Compared with the linear array CCD, it has the advantages of high responsiveness, large dynamic range, and high signal to noise ratio [1–5]. For the ordinary CCD, there is a contradiction between the target moving speed and the exposure time. The TDI CCD is an excellent solution to the problem, which can be high-speed target imaging, while at the same time enhancing the exposure time. Its higher responsiveness can reduce the relative aperture of the optical system and, thus, reduce the weight and volume of aerospace remote sensors, which is very suitable for use in the field of space remote sensing [6–8].

In the aerial camera imaging, it is necessary to keep the TDI CCD charge transfer speed consistent with the moving speed of the target on the focal plane in order to correctly extract the target image information [9]. In practical application, the charge transfer frequency of the TDI CCD is usually calculated based on the information of the orbit and attitude parameters of the satellite remote sensing platform, and the matching relationship is guaranteed [10,11].

The modulation transfer function (MTF) shows the relation between image contrast and spatial frequency when the sensor collects images. At the same time, MTF is commonly used for evaluating the quality of the sensor's performance [12–15]. Therefore, the MTF in the scanning direction and the MTF in the cross-scan direction are taken as an index to measure the image quality in this paper.

The MTF of the obtained image in the scanning direction is usually lower than the MTF in the cross-scan direction. As aerospace camera imaging is a dynamic push-broom process, so many error factors can lead to the decline of the image quality in the scanning direction [16–19]. Yanlu Du mainly analyzed the impact of sinusoidal vibration on dynamic MTF [20]. The theoretical model of MTF and quantum efficiency based on the CCD and complementary metal–oxide–semiconductor (CMOS) detectors was established by Ibrahima Djite, which was mainly aimed at the factors of pixel size and charge diffusion [21]. Xiaowei Shi established an MTF model for TDI detectors using oversampling-superposition technology, and the

negative effects of different velocity mismatch ratios on MTF were analyzed at the same time. But, the model only carried out the simulation analysis without experimental verification [22].

Steven L. Smith described the causes of the loss of image quality in high-resolution remote sensing systems and pointed out the factors that cause image blurring, including geometric smear, clocking smear, terrain smear, and smear from optical distortions. The drop of the MTF in the scanning direction caused by integer pixels smear was also analyzed. However, the model was analyzed in terms of the line transfer period, and the specific charge transfer process was not analyzed. So, this element was also neglected in the model [23].

Kaiming Nie proposed an analytical model of MTF for a TDI CMOS image sensor (TDI-CIS) in the scanning direction. The pixel value sensitive ratio and velocity mismatch were analyzed in the literature, and the influence of integral series on velocity mismatch was considered. The charge transfer process in the line period was also considered in the model, but, in the case of the charge readout, the TDI CMOS is different from the TDI CCD, which means that the analysis cannot apply to the TDI CCD [24].

By analyzing the charge transfer process of a typical three-phase TDI CCD, Dejiang Wang pointed out the reason for the charge transfer image shift and then proposed an improved driving timing method to improve the MTF in the scanning direction. But, the timing is based on the TDI CCD with a special architecture, which cannot be applied to the traditional TDI CCD [25].

The abovementioned literature analyzes the impact of the MTF from multiple aspects, including geometric smear, clocking smear, terrain smear, and vibration smear. But, there are few models that take into account the image shift introduced by the multi-phase step-by-step charge transfer process in the charge line transfer period, which we call the charge transfer image shift.

In this paper, the charge transfer image shift model is established for the process of charge transfer in the line period, and the method of reducing the charge transfer image is proposed. The method has been experimentally verified. The remainder of this paper is organized as follows: the cause of the charge transfer image shift is analyzed in Section 2. The charge transfer image shift model is established for the process of charge transfer in the line period in Section 3. In Section 4, typical simulation results are presented, and the key parameter, which has an impact on MTF, is analyzed. An improved driving timing is proposed in Section 5. The theoretical analysis is experimentally verified in Section 6. Section 7 gives the conclusions.

2. CHARGE TRANSFER IMAGE SHIFT ANALYSIS

Compared with an ordinary CCD, TDI CCD introduced a time delay integral technology, improving the responsiveness and signal to noise ratio, but it also put forward stringent requirements in the application conditions. First, the direction of the target movement must be consistent with the direction of the integration of the TDI CCD, that is the direction of the photogenerated charge packet transfer. Second, the velocity of the target on the focal plane must be consistent with the transfer rate of the TDI CCD photogenerated packet. In the aerial camera imaging, the target image is a continuous motion on the focal plane, while the photogenerated charge packet is a discrete step-by-step motion driven by the TDI CCD pulse timing. The charge transfer line frequency can only guarantee the average speed matching, which is calculated according to the orbit and attitude parameters of the satellite platform, and there is still the image shift caused by the charge step-by-step transfer in the line period. This is one of the reasons that caused the MTF of the majority of aerospace cameras in the scanning direction to be lower than the theoretical value.

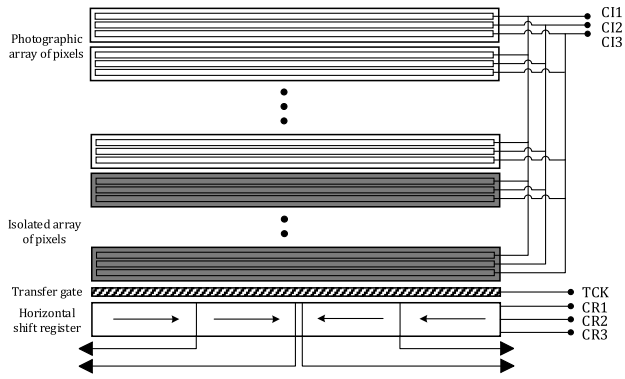

Fig. 1. Typical structure of the three-phase TDI CCD.

The TDI CCD can be divided into two phases, three phases, and four phases, according to the number of electrodes within the pixel, which have the same basic working principle. The three-phase TDI CCD is analyzed as an example.

As Fig. 1 shows, the TDI CCD consists of a photographic array of pixels, an isolated array of pixels, a transfer gate, and a horizontal shift register. The electrodes of photographic array and isolated array are driven by the image region clock (CI1, CI2, and CI3) signals to complete the vertical transfer of charge from the top to the bottom. The transfer gate is driven by the transfer clock (TCK) signal to transfer the charge in the isolated array to the horizontal shift register, while blocking aliasing of the charge between the isolated array and the horizontal shift register. The charge in the horizontal shift register is quantized and read out one by one, driven by readout clock (CR1, CR2, and CR3) signals.

As Fig. 2 shows, the last two lines of isolated pixels are taken for analysis, where T1–T6 are the different times within the line transfer period. In the T1–T2 period, the CI1 and CI2 signals remain high to form a charge potential well, the CI3 signal remains low to form a charge barrier, and a photogenerated charge is collected under the electrodes of the CI1 and CI2 signals. In the T2–T3 period, the CI2 signal remains high to form a charge potential well, the CI1 and CI3 signals remain low to form a charge barrier, and the photogenerated charge is collected under the electrode of the CI2 signal. After six periods of this type, at time T1, the charge transfer of one line is completed. The TCK signal goes low to form a charge barrier, isolating the charge in the horizontal shift register. In the T1–T2 period, the charge in the horizontal shift register is shifted out; at time T2, the TCK returns to high,

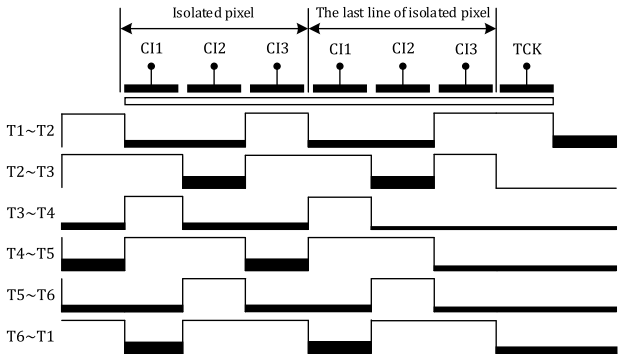

Fig. 2. Process of charge transfer in a line period.

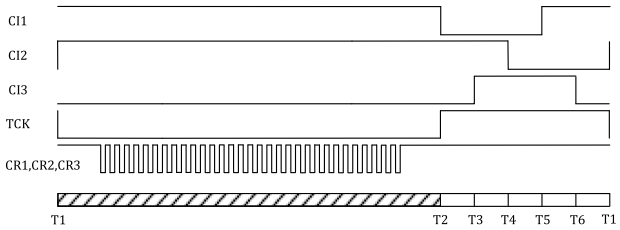

Fig. 3. Timing diagram of the three-phase TDI CCD.

and the transfer gate is turned on again to receive the transfer charge of the next line.

By analyzing the transfer process of the three-phase TDI CCD, it can be seen that the charge transfer can be divided into six stages in a line transfer period, that is the line driving signals CI1, CI2, and CI3 are divided into six steps to complete the transfer of charge. In the T1–T2 period, it is necessary to start the CR signals to read out the charge in the horizontal shift register, which takes a certain amount of time, so this period is usually much longer than that of other periods. Figure 3 shows the three-phase TDI CCD specific drive signal timing.

Under the condition that the line period of the TDI CCD matches the target moving speed on the focal plane, and the three-phase TDI CCD is driven according to the timing shown in Fig. 3, the contrast curve of the target image displacement and the transferred charge displacement is shown in Fig. 4.

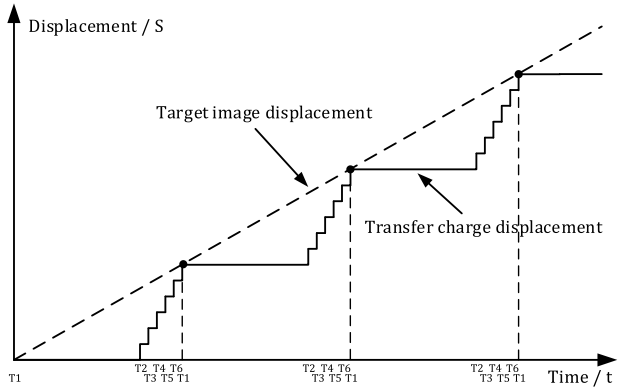

Fig. 4. Contrast curve of the target image displacement and the transferred charge displacement.

3. ESTABLISHMENT OF CHARGE TRANSFER IMAGE SHIFT MODEL

The evaluation of the imaging quality of the optical system using the optical transfer function (OTF) is based on the idea that the target is composed of spectra of various frequencies. If the optical system is a linear time-invariant system, then, after the transmission of the optical system, the variation of the amplitude and phase with the spatial frequency is called the OTF. The modulus of the OTF is the MTF, which is an important indicator to evaluate the imaging quality of the optical system. In the case of sinusoidal input signals, it is defined as the ratio of the output contrast $C_o\ (f)$ to the input contrast $C_i\ (f)$ [26–28]:

$$\mathrm{MTF} = C_o(f)/C_i(f), \tag{1}$$

while the contrast is defined as

$$C(f) = \frac{L_{\max} - L_{\min}}{L_{\max} + L_{\min}}, \tag{2}$$

where $L_{\max}$ and $L_{\min}$ are the maximum and minimum values of light intensity, respectively.

Based on the definition of MTF, the decrease of MTF caused by the discrete sampling of pixels will be analyzed. During the photoelectric conversion of the CCD, the decrease of MTF caused by the discrete sampling of pixels is defined as the variable MTF_D.

It is assumed that the focal plane of the TDI CCD is irradiated by the optical signal $O\ (x, y)$, which is sinusoidal along the x-axis direction with a spatial frequency f and constant in the y-axis direction, as shown in Fig. 5. The light intensity can be expressed as follows:

$$O(x, y) = A[1 + \sin(2\pi f x)], \tag{3}$$

where A is the magnitude of the light intensity.

Take one of the pixels on the CCD, and the coordinates of the pixel center are (x_p, x_p). The energy $E\ (x_p, y_p)$ obtained by the pixel in the integration time t can be expressed as

$$E(x_p, y_p) = \int_0^t \int_{y_p - \frac{d}{2}}^{y_p + \frac{d}{2}} \int_{x_p - \frac{d}{2}}^{x_p + \frac{d}{2}} A[1 + \sin(2\pi f x)]\mathrm{d}x\mathrm{d}y\mathrm{d}t. \tag{4}$$

The above formula can be further organized as

$$E(x_p, y_p) = t \cdot d \cdot A\left[d + \frac{1}{\pi f}\ \sin(2\pi f x_p) \cdot \sin(\pi f d)\right]. \tag{5}$$

The contrast of the input and output signals can be calculated as follows:

$$C_i(f) = \frac{2A - 0}{2A + 0} = 1, \tag{6}$$

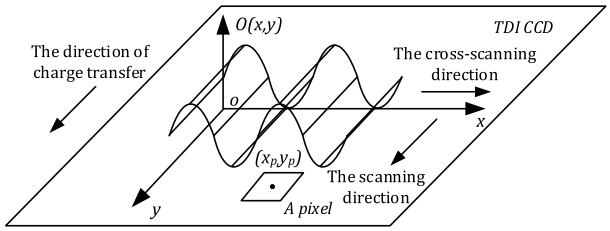

Fig. 5. Diagram of the light intensity of the input signal.

$$C_o(f) = \frac{t \cdot d \cdot A\left[d + \frac{\sin(\pi f d)}{\pi f}\right] - t \cdot d \cdot A\left[d - \frac{\sin(\pi f d)}{\pi f}\right]}{t \cdot d \cdot A\left[d + \frac{\sin(\pi f d)}{\pi f}\right] + t \cdot d \cdot A\left[d - \frac{\sin(\pi f d)}{\pi f}\right]} = \frac{\sin(\pi f d)}{\pi f d}. \quad (7)$$

So, the decrease of MTF caused by the discrete sampling of pixels can be calculated as follows:

$$\mathrm{MTF}_D = \frac{C_o(f)}{C_i(f)} = \frac{\sin(\pi f d)}{\pi f d}, \quad (8)$$

where f is the spatial frequency of the optical signal, and d is the pixel size of the CCD detector. Its value at the Nyquist frequency is 0.6366, which is the ideal MTF in the cross-scan direction.

Assuming that the phase number of the TDI CCD is n ($n = 2, 3, 4$), the ratio of the T1–T2 periods occupying the entire line transfer period T in Fig. 1 is defined as D_{CR}, and the proportion of the remaining time to the line period is defined as D_{CI}; then, there is $D_{\mathrm{CR}} + D_{\mathrm{CI}} = 1$. The whole period of charge transfer can be divided into $T \times D_{\mathrm{CR}}$, $T \times D_{\mathrm{CI}}/(2n-1)$, and $T \times D_{\mathrm{CI}}/(2n-1)\ldots(A$ total of $2n)$. The position of the transfer charge in different periods is shown in Fig. 6.

It is assumed that the focal plane of the TDI CCD is irradiated by the optical signal $O(x, y)$, which is sinusoidal along the y-axis direction with a spatial frequency f, constant in the x-axis direction, and it moves at a constant speed v along the y axis, as shown in Fig. 7. The light intensity can be expressed as follows:

$$O(x, y) = A[1 + \sin(2\pi f(y - vt))], \quad (9)$$

where A is the magnitude of the light intensity.

Take one of the pixels on the CCD, and the coordinates of the pixel center are (x_p, x_p). Considering the process of charge transfer, the energy $E_{\mathrm{sum}}(x_p, y_p)$ obtained by the pixel in a line period T can be calculated as follows.

The energy $E_1(x_p, y_p)$ obtained from T1 to T2 is

$$E_1(x_p, y_p) = \int_0^{T \cdot D_{\mathrm{CR}}} \int_{y_p - \frac{d}{2}}^{y_p + \frac{d}{2}} \int_{x_p - \frac{d}{2}}^{x_p + \frac{d}{2}} A[1 + \sin(2\pi f(y - vt))]\mathrm{d}x\mathrm{d}y\mathrm{d}t. \quad (10)$$

Since the distance of the target moving on the focal plane in a line period T is a pixel size d, there is

$$vT = d. \quad (11)$$

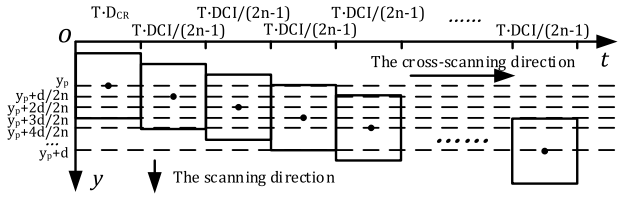

Fig. 6. Position diagram of the transfer charge.

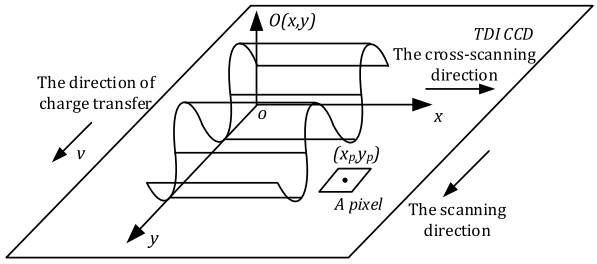

Fig. 7. Diagram of the light intensity of the input signal.

Then, the above formula can be further organized as

$$E_1(x_p, y_p) = d \cdot A\left\{d \cdot T \cdot D_{\mathrm{CR}} + T \cdot \frac{\sin(\pi f d)}{2\pi^2 f^2 d}[\cos(2\pi f(y_p - d \cdot D_{\mathrm{CR}})) - \cos(2\pi f y_p)]\right\}. \quad (12)$$

Similarly, the energy $E_2(x_p, y_p)$ obtained from T2 to T3 is

$$E_2(x_p, y_p) = d \cdot A\left\{d \cdot T \cdot \frac{D_{\mathrm{CI}}}{2n-1} + T \cdot \frac{\sin(\pi f d)}{2\pi^2 f^2 d} \times \left[\cos\left(2\pi f\left(y_p + 2 \cdot \frac{d}{2n} - d \cdot \left(D_{\mathrm{CR}} + \frac{2D_{\mathrm{CI}}}{2n-1}\right)\right)\right) - \cos\left(2\pi f\left(y_p + 2 \cdot \frac{d}{2n} - d \cdot \left(D_{\mathrm{CR}} + \frac{D_{\mathrm{CI}}}{2n-1} D_{\mathrm{CI}}\right)\right)\right)\right]\right\}. \quad (13)$$

In this way, the energy $E_{\mathrm{sum}}(x_p, y_p)$ obtained by the pixel in line period T is the accumulation of each time period:

$$E_{\mathrm{sum}}(x_p, y_p) = \sum_{i=1}^{2n} E_i(x_p, y_p). \quad (14)$$

The output signal contrast $C_o(f)$ can be obtained by calculating the maximum and minimum values for $E_{\mathrm{sum}}(x_p, y_p)$, and the input signal contrast $C_i(f)$ is known as one; thereby, the decrease of MTF due to the charge transfer image shift is obtained, which is defined as the variable MTF_S.

4. ANALYSIS OF MTF OPTIMIZATION

Based on the above model, the calculation of the specific TDI CCD parameters is carried out. Taking the three-phase TDI CCD as an example, assuming that the D_{CR} is 50%, then the D_{CI} is 50%, and the line transfer period T can be divided into 0 to $0.5T$, $0.5T$ to $0.6T$, $0.6T$ to $0.7T$, $0.7T$ to $0.8T$, $0.8T$ to $0.9T$, and $0.9T$ to T. The energy obtained at each period is given by

$$E_1(x_p, y_p) = d \cdot A\left\{d \cdot T \cdot 0.5 + T \cdot \frac{\sin(\pi f d)}{2\pi^2 f^2 d} \times [\cos(2\pi f(y_p - 0.5d)) - \cos(2\pi f y_p)]\right\}, \quad (15)$$

$$E_2(x_p, y_p) = d \cdot A\left\{d \cdot T \cdot 0.1 + T \cdot \frac{\sin(\pi f d)}{2\pi^2 f^2 d}\left[\cos\left(2\pi f\left(y_p - \frac{13}{30}d\right)\right) - \cos\left(2\pi f\left(y_p - \frac{1}{3}d\right)\right)\right]\right\}, \tag{16}$$

$$E_3(x_p, y_p) = d \cdot A\left\{d \cdot T \cdot 0.1 + T \cdot \frac{\sin(\pi f d)}{2\pi^2 f^2 d}\left[\cos\left(2\pi f\left(y_p - \frac{11}{30}d\right)\right) - \cos\left(2\pi f\left(y_p - \frac{4}{15}d\right)\right)\right]\right\}, \tag{17}$$

$$E_4(x_p, y_p) = d \cdot A\left\{d \cdot T \cdot 0.1 + T \cdot \frac{\sin(\pi f d)}{2\pi^2 f^2 d}[\cos(2\pi f(y_p - 0.3d)) - \cos(2\pi f(y_p - 0.2d))]\right\}, \tag{18}$$

$$E_5(x_p, y_p) = d \cdot A\left\{d \cdot T \cdot 0.1 + T \cdot \frac{\sin(\pi f d)}{2\pi^2 f^2 d}\left[\cos\left(2\pi f\left(y_p - \frac{7}{30}d\right)\right) - \cos\left(2\pi f\left(y_p - \frac{2}{15}d\right)\right)\right]\right\}, \tag{19}$$

$$E_6(x_p, y_p) = d \cdot A\left\{d \cdot T \cdot 0.1 + T \cdot \frac{\sin(\pi f d)}{2\pi^2 f^2 d}\left[\cos\left(2\pi f\left(y_p - \frac{1}{6}d\right)\right) - \cos\left(2\pi f\left(y_p - \frac{1}{15}d\right)\right)\right]\right\}. \tag{20}$$

When the spatial frequency f is $1/2d$, which is the Nyquist frequency,

$$E_{\text{sum}}(x_p, y_p) = d \cdot A\left\{d \cdot T + T \cdot \frac{\sin(\pi f d)}{2\pi^2 f^2 d} \cdot 2.05824 \cdot [\sin(2\pi f y_p) - \cos(2\pi f y_p)]\right\}. \tag{21}$$

Then, the output signal contrast $C_o(f)$ is obtained as follows:

$$C_o(f) = \frac{d \cdot A\left\{d \cdot T + T \cdot \frac{\sin(\pi f d)}{2\pi^2 f^2 d} \cdot 2.05824 \cdot \sqrt{2}\right\} - d \cdot A\left\{d \cdot T + T \cdot \frac{\sin(\pi f d)}{2\pi^2 f^2 d} \cdot 2.05824 \cdot (-\sqrt{2})\right\}}{d \cdot A\left\{d \cdot T + T \cdot \frac{\sin(\pi f d)}{2\pi^2 f^2 d} \cdot 2.05824 \cdot \sqrt{2}\right\} + d \cdot A\left\{d \cdot T + T \cdot \frac{\sin(\pi f d)}{2\pi^2 f^2 d} \cdot 2.05824 \cdot (-\sqrt{2})\right\}} \approx 0.5899. \tag{22}$$

Eventually, the MTF_s is obtained under the following condition:

$$\text{MTF}_s = \frac{C_o(f)}{C_i(f)} \approx 0.5899 \quad (n = 3, D_{\text{CR}} = 50\%, f = 1/2d). \tag{23}$$

According to the method above, a cluster of curves that the MTF in the scanning direction varies with the target spatial frequency are plotted in Fig. 8, when D_{CR} has different values. The spatial frequency of the horizontal axis in the figure has been normalized.

It can be seen from the curves that there are differences between the MTF curves at different D_{CR} values, proving that the D_{CR} value does have an effect on the MTF in the scanning direction. When the D_{CR} is the maximum value of 90%, the MTF at the Nyquist frequency is 0.4512. When the D_{CR} is the minimum value of 5%, the MTF at the Nyquist frequency is 0.6245.

In order to analyze the influence of the D_{CR} value on the MTF in the scanning direction, the relationship between the D_{CR} value and the MTF at the Nyquist frequency is shown in Fig. 9, where the horizontal axis is the D_{CR} value, and the vertical axis is the MTF value.

It can be seen from the figure that they are not linearly related, so with the increase of D_{CR}, the MTF value increases first and then decreases. The MTF is 0.6354 at the D_{CR} equal to 16.67% of the line period, which corresponds to be the case

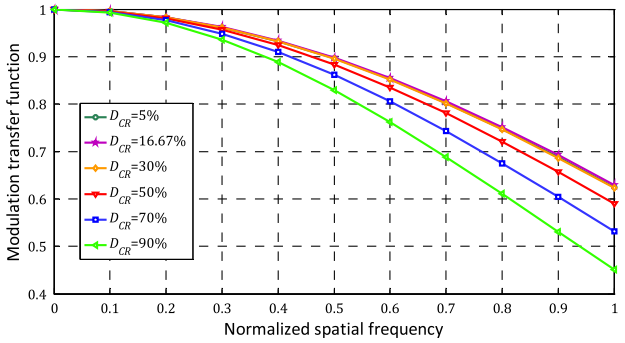

Fig. 8. Relationship between the MTF in the scanning direction and target spatial frequency.

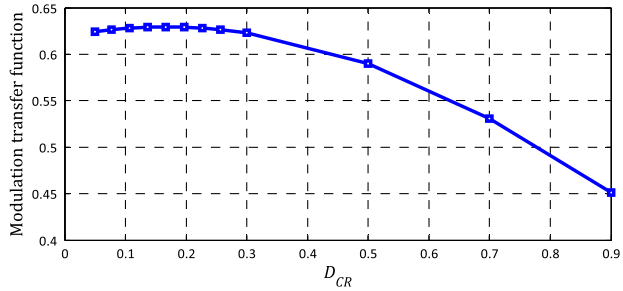

Fig. 9. Relationship between the MTF in the scanning direction and the parameter D_{CR}.

of CI signals equally spaced. This value is already very close to the value of the MTF in the cross-scan direction, which is theoretically 0.6366. So, the realization of equal space of CI signals is the key to enhance MTF in the scanning direction.

5. IMPROVEMENT OF TDI CCD TIMING

Considering the actual working process of the TDI CCD, the CR signals must be left enough time to guarantee that the charge in the horizontal shift register is completely read out. In practical systems, the CR signals usually take up most of the time in a line period, which makes it difficult to implement the maximum value of MTF in the scanning direction, that is, the CI signals are equally spaced. In view of the above problem, we propose an improved TDI CCD driving timing.

Figure 10 shows the improved driving timing of three-phase TDI CCD, where T1–T6 are equal intervals in a line period. The improved CI signals are equally spaced in six stages, and the timing relationship between the TCK signal and CI signals is adjusted. During the time T1–T5, the TCK signal is maintained at a low level to form a charge barrier, which isolates the vertically shifted charge, and the charge to be read out in the horizontal shift register, avoiding the charge aliasing. The period between T1 and T5 occupies two-thirds of the entire line period, leaving the CR signals enough time to complete the readout of the charge.

Figure 11 shows the process of charge transfer based on the timing of the driving signal in Fig. 10. In contrast to the traditional process of the three-phase TDI CCD charge transfer in Fig. 2, the TCK signal remains low for T2–T5, constituting a charge barrier. It can be seen from the process of charge transfer that the charge barrier formed by the TCK signal in this period does not affect the line transfer of the charge, so this timing is feasible in principle.

6. EXPERIMENTAL RESULTS

The experimental system is established to verify the results of the theoretical analysis above. Figure 12 shows the basic composition of the experimental system, which mainly consists of a three-phase TDI CCD detector and drive circuit components, optical lens, dynamic target generator, host computer, and optical vibration isolation platform. In order to reduce external shock during the imaging process, the whole system is placed on the isolation platform, in which the target moving direction of the dynamic target generator is placed in the same direction as the TDI CCD charge transfer direction.

The pixel size of the CCD used in the experiment is 8.75 μm, and the corresponding space Nyquist frequency is

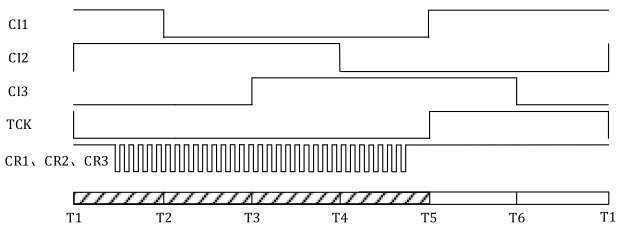

Fig. 10. Improved timing diagram of the three-phase TDI CCD.

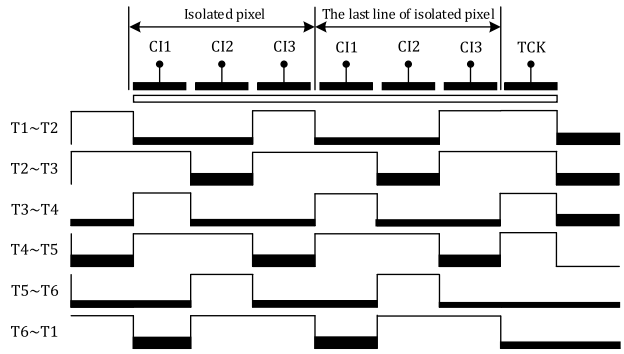

Fig. 11. Process of improved charge transfer in a line period.

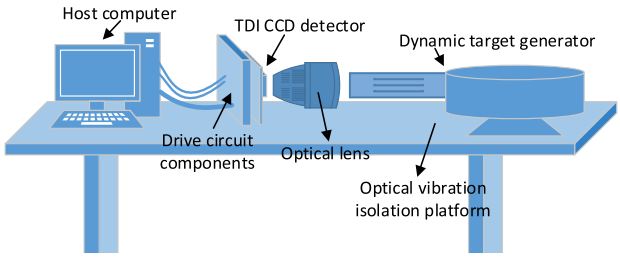

Fig. 12. Composition of the experimental system.

57.14 lines/mm. The system parameters are adjusted so that the target selected for the experiment has a corresponding spatial resolution of 57.14 to 10 lines/mm on the focal plane of the CCD, which makes it easier to observe the lifting effect of the MTF.

The images of the target obtained by setting the different D_{CR} values by adjusting the CI signals are shown in Fig. 13. Wherein, the vertical direction in the figure is the scanning direction, and the horizontal direction is the cross-scanning direction. Due to the restriction of the CR readout signals, the minimum value of D_{CR} achievable in the experimental conditions is 50% when driving with traditional timing. Therefore, the D_{CR} values in Figs. 13(a)–13(c) are set to 90%, 70%, and 50%, respectively, and the D_{CR} value in Fig. 13(d) is 16.67%, using the improved drive timing.

The TDI CCD scans the target along the vertical direction of Fig. 13, in which we can clearly see that the longitudinal target bars have substantially the same sharpness, and the transverse target bars have a better clarity and contrast from Figs. 13(a)–13(c). Figure 13(d), which uses the improved timing, has the best imaging effect.

The curves of the MTF in the scanning direction at different D_{CR} values are calculated from the above target images, as shown in Fig. 14, and the MTF curve in the cross-scan direction can be referenced as a static MTF. It can be seen from Fig. 14 that the MTF curves are gradually shifted up during the D_{CR} value decrease from 90% to 50%. The measured MTF values at the Nyquist frequency are 0.133, 0.151, and 0.176, respectively. When the improved timing is used, the MTF in the scanning direction at the Nyquist frequency is 0.189, which is close to 0.191 of the static MTF.

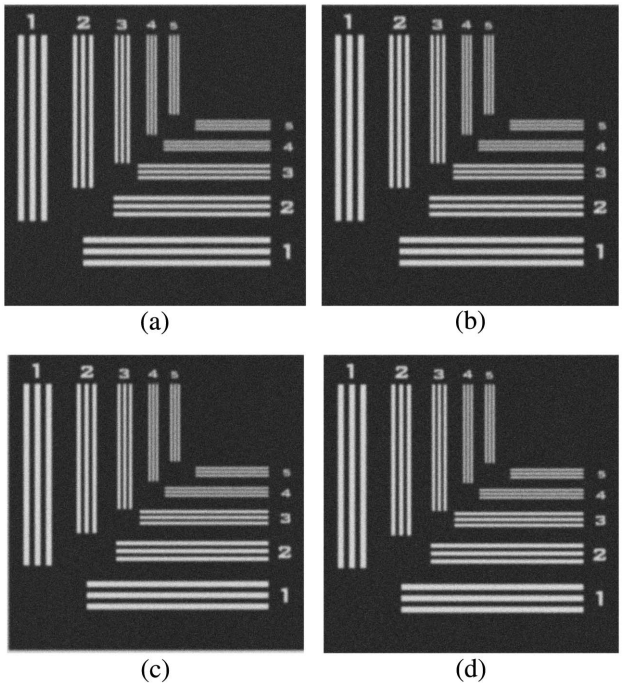

Fig. 13. Target images obtained at different D_{CR} values (a) when the D_{CR} is 90% with traditional timing, (b) when the D_{CR} is 70% with traditional timing, (c) when the D_{CR} is 50% with traditional timing, and (d) when the D_{CR} is 16.67% with the improved timing.

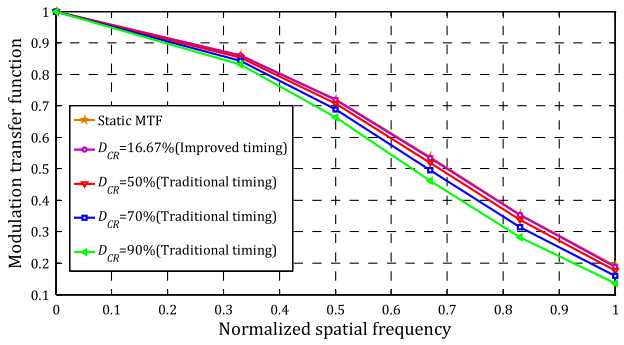

Fig. 14. Curves of the MTF test results at different D_{CR} values.

So, we can enhance the MTF in the scanning direction by adjusting the D_{CR} value. With the improved timing, the MTF in the scanning direction is close to the MTF in the cross-scan direction.

7. CONCLUSIONS

In the process of the remote sensing camera scanning the ground, which uses the TDI CCD as the sensor, usually the MTF of the acquired image in the scanning direction is lower than the MTF in the cross-scan direction. In addition to the error factor of the TDI CCD charge transfer frequency and target movement speed, it is also closely related to the transfer timing of the charge in a line period.

Based on the theoretical model and experimental verification, it is proved that on the basis of the existing TDI CCD architecture and driving method, the MTF in the scanning direction can be raised by adjusting the CI signals, and there is a maximum value near the MTF value in the cross-scan direction, which corresponds to the case of CI signals being equally spaced.

In the actual system, by adjusting the TCK signal and improving the driving timing of the TDI CCD, it is possible to realize the equal interval distribution of CI signals in a line period, which can significantly improve the MTF in the scanning direction.

Funding. People's Government of Jilin Province (20150312039ZG).

REFERENCES

1. B. Zhao and B. He, "Description of TDI-CCD remote sensing image," in *3rd International Conference on Advanced Computer Theory and Engineering (ICACTE)* (2010), Vol. **6**, pp. 325–328.
2. M. R. Sajan, C. J. Tay, H. M. Shang, and A. Asundi, "Scanning moiré and phase shifting with time delay and integration imaging," Opt. Lett. **22**, 1281–1283 (1997).
3. A. Eckardt and R. Reulke, "New detectors and detector architectures for high resolution optical sensor systems," in *Seventh International Conference on Sensing Technology (ICST)* (2013), pp. 645–649.
4. H. S. Wong, Y. L. Yao, and E. S. Schlig, "TDI charge-coupled devices: design and applications," IBM J. Res. Dev. **36**, 83–106 (1992).
5. M.-H. Gao, G.-J. Zhao, L. Liu, and J.-Y. Ren, "Study on dynamic imaging on TDI CCD optical remote sensor of push-broom technology," Proc. SPIE **7656**, 76567B (2010).
6. D. Robinson, "Computational imaging approaches, challenges and R&D opportunity in the earth-imaging remote sensing industry," in *Imaging and Applied Optics Congress* (2016), paper CTH3B.1.
7. Z. Sun, L. Zhang, G. Jin, and X. Yang, "Design of ground-based physical simulation system for satellite-borne TDI-CCD dynamic imaging," Proc. SPIE **7850**, 785014 (2010).
8. S. Tao, G. Jin, X. Zhang, H. Qu, and Y. An, "Wavelet power spectrum-based autofocusing algorithm for time delayed and integration charge coupled device space camera," Appl. Opt. **51**, 5216–5223 (2012).
9. S. W. Li, T. J. Liu, and H. Q. Wang, "Image mosaic for TDICCD push-broom camera image based on image matching," Remote Sens. Technol. Appl. **24**, 374–378 (2009).
10. S.-F. Tong, J.-G. Liu, J. Ruan, and Z. Hao, "An analysis for application technique of push-broom TDI-CCD imaging camera," Opto-Electron. Eng. **23**, 31–33 (2001).
11. J. Wang, P. Yu, C. Yan, J. Ren, and B. He, "Space optical remote sensor image motion velocity vector computational modelling, error budget and synthesis," Chin. Opt. Lett. **3**, 414–417 (2005).
12. G. Li, W. Wang, H. Li, L. Jin, and Y. Liu, "The research of the accurate measure of static transfer function for the TDI CCD camera," Proc. SPIE **8332**, 83320Z (2011).
13. B. M. Lambert and J. M. Harbold, "Experimental methods for measurement of the modulation transfer function (MTF) for time-delay-and-integrate (TDI) charge coupled device (CCD) image sensors," Proc. SPIE **7405**, 74050M (2009).
14. D. N. Sitter, J. S. Goddard, and R. K. Ferrell, "Method for the measurement of the modulation transfer function of sampled imaging systems from bar-target patterns," Appl. Opt. **34**, 746–751 (1995).
15. D. Xu and X. Zhang, "Study of MTF measurement technique based on special object image analyzing," in *IEEE International Conference on Mechatronics and Automation* (2012), pp. 2109–2113.
16. Z. Lin, "Synchronous error analysis of dynamic imaging based on TDI-CCD optical targets," Semicond. Optoelectron. **30**, 316–319 (2009).
17. K. Madanipour and M. T. Tavassoly, "Determination of modulation transfer function of a printer by measuring the autocorrelation of

the transmission function of a printed Ronchi grating," Appl. Opt. **48**, 725–729 (2009).
18. W. Dejiang, K. Haipeng, and C. Xichang, "Digital implementation of forward motion compensation in TDI-CCD panoramic aerial camera," Opt. Precis. Eng. **16**, 2465–2472 (2008).
19. P. Jain, "One-dimensional sensor modulation transfer function, revisited," Appl. Opt. **54**, D33–D37 (2015).
20. Y. Du, Y. Ding, Y. Xu, and C. Sun, "Dynamic modulation transfer function analysis of images blurred by sinusoidal vibration," J. Opt. Soc. Korea **20**, 762–769 (2016).
21. I. Djite, M. Estribeau, P. Magnan, G. Rolland, S. Petit, and O. Saint-Pe, "Theoretical models of modulation transfer function, quantum efficiency, and crosstalk for CCD and CMOS image sensors," IEEE Trans. Electron. Dev. **59**, 729–737 (2012).
22. X. Shi, X. Wu, and X. Xu, "Modulation transfer function model of scanning TDI sensors with oversampling-superposition," in *IEEE International Instrumentation and Measurement Technology Conference* (2008).
23. S. L. Smith, J. Mooney, T. A. Tantalo, and R. D. Fiete, "Understanding image quality losses due to smear in high-resolution remote sensing imaging systems," Opt. Eng. **38**, 821–826 (1999).
24. K. Nie, L. Li, S. Yao, and J. Xu, "Scanning modulation transfer function model of TDI CMOS image sensor," J. Signal Process. Syst. **82**, 17–25 (2016).
25. D. Wang, T. Zhang, and H. Kuang, "Clocking smear analysis and reduction for multiphase TDI CCD in remote sensing system," Opt. Express **19**, 4868–4880 (2011).
26. E. G. Stevens, "A unified model of carrier diffusion and sampling aperture effects on MTF in solid-state image sensors," IEEE Trans. Electron. Dev. **39**, 2621–2623 (1992).
27. J. F. Johnson, "Modeling imager deterministic and statistical modulation transfer functions," Appl. Opt. **32**, 6503–6513 (1993).
28. S. M. Backman, A. J. Makynen, T. T. Kolehmainen, and K. M. Ojala, "Random target method for fast MTF inspection," Opt. Express **12**, 2610–2615 (2004).